

HEADREST OR HORSE BIT VFIG 2003.7 - LEADED BRONZE - MODERN TIMES

Artefact name Headrest or horse bit VFig 2003.7

Authors Christian. Degrigny (HE-Arc CR, Neuchâtel, Neuchâtel, Switzerland) & Valentin. Boissonnas (HE-Arc CR, Neuchâtel, Neuchâtel, Switzerland)

Url /artefacts/395/

✧ The object



Fig. 1: Headrest or horse bit, side and front view,

Credit HE-Arc CR_N.Barbezat.

✧ Description and visual observation

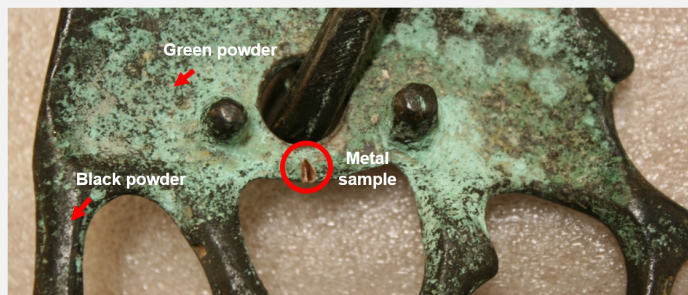
Description of the artefact	Artefact made of two figurative (winged wild sheep) plates attached by a central bar (Fig. 1). One of the volutes of the bar is filled with metal suggesting it was cast with its end rolled up already. The surfaces of the plates (both sides) and the central bar are covered with a black adherent layer. A heterogeneous green layer is visible over this black layer. Well adhering hard brown-grey sediment-like deposits are present mostly in the middle of the plates on both sides. Red and orange spots are unevenly distributed on the surface (white arrow). Dimensions: W plates = 13mm; H plates = 105mm, L bar = 185mm, WT = 925g.
Type of artefact	Headrest or horse bit
Origin	Luristan (?)
Recovering date	Date unknown
Chronology category	Modern Times
chronology tpq	<input type="text" value="1000"/> B.C. ▾
chronology taq	<input type="text" value="650"/> B.C. ▾
Chronology comment	Between 1000 and 650 years BC (if original) or 20th century (if fake)
Burial conditions / environment	Unknown
Artefact location	Bible & Orient Museum, Fribourg, Fribourg
Owner	Bible & Orient Museum, Fribourg, Fribourg

Inv. number	VFig 2003.7
Recorded conservation data	Not conserved

Complementary information

Nothing to report.

Study area(s)

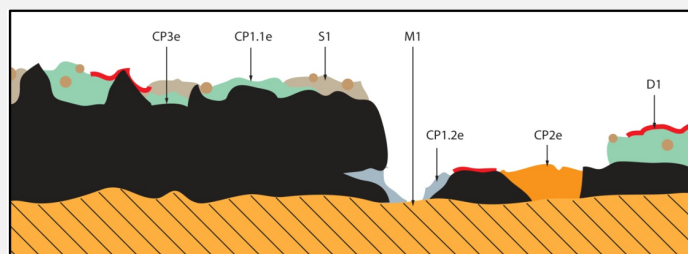


Credit HE-Arc CR_N.Barbezat.

Fig. 2: Location of sampling areas,

Binocular observation and representation of the corrosion structure

The schematic representation below gives an overview of the corrosion layers encountered on the object from visual macroscopic observation (additional e and i within the coding correspond to strata in contact with the environment (e) and internal strata (i)).



S1: soil (sand and limestone)
D1: red deposit
CP1.1e: outer light green-blue corrosion layer
CP1.2e: outer white-blue-grey corrosion layer
CP2e: outer orange corrosion layer
CP3e/i: outer/inner black brown corrosion layer
M1: metal

Credit HE-Arc CR, N.Barbezat.

Fig. 3: Stratigraphic representation of the artefact in cross-section by macroscopic observation,

MiCorr stratigraphy(ies) – Bi

Sample(s)

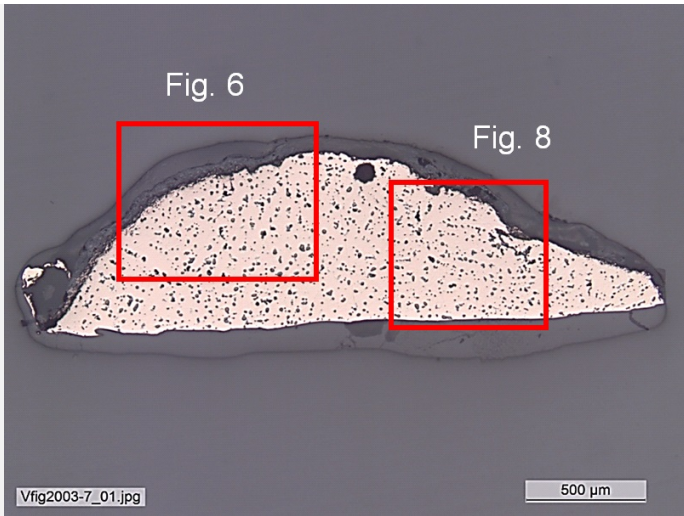


Fig. 4: Micrograph of the cross-section of sample from Fig. 2 showing the location of Figs. 6 and 8,

Credit HE-Arc CR.

Description of sample	The sample was cut on the bottom of one of the plates (Fig. 2). On Fig. 4, the top and round shape of the sample is the outer part of the metal. It is covered with corrosion layers. The lower part of the sample corresponds to the cut metal with no corrosion products.
Alloy	Leaded Bronze
Technology	Cast and cold worked (with final annealing?)
Lab number of sample	None
Sample location	HE-Arc CR, Neuchâtel, Neuchâtel
Responsible institution	Bible & Orient Museum, Fribourg, Fribourg
Date and aim of sampling	2014, metallography and chemical analyses

Complementary information

Nothing to report.

∨ Analyses and results

Analyses performed:

Metallography (etched with ferric chloride reagent), SEM/EDS and FTIR.

∨ Non invasive analysis

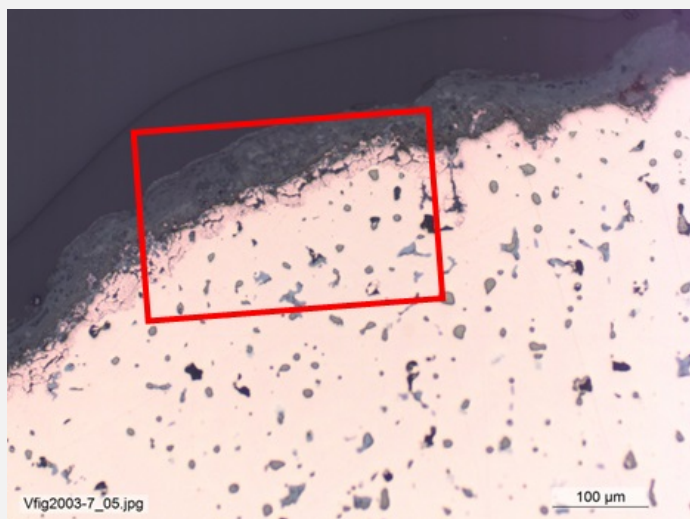
∨ Metal

The remaining metal is a leaded bronze (Table 1) containing numerous copper sulphide and lead (Pb) inclusions (Figs. 6 and 7). The porosity is difficult to distinguish since the pores seem to have similar dimensions as the inclusions that could have been removed during the polishing of the sample (Fig. 6). After etching, the structure of the metal appears to be made up mostly of dendrites, but a grain structure seems to have developed on the right side of the sample, with occasional twin lines (Figs. 8 and 9). The twinned grain

structure could be the result of cold work and annealing after casting, possibly through the application of an artificial patina under heat.

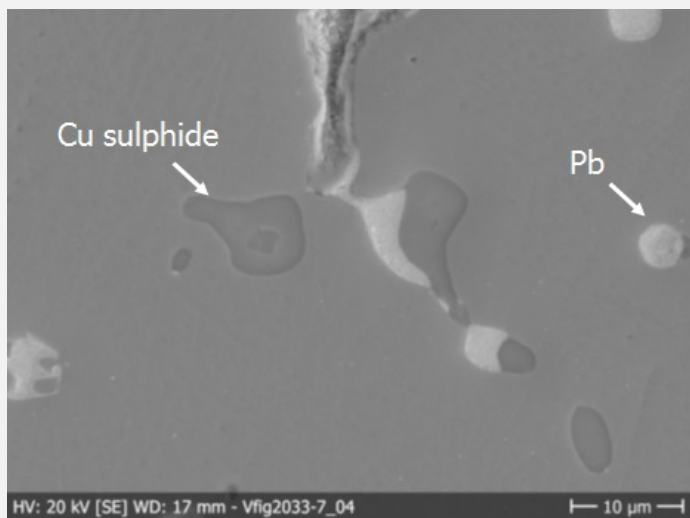
Elements	Cu	Sn	Pb
mass%	85	7	5

Table 1: Chemical composition of the metal. Method of analysis: SEM-EDS, Lab of Electronic Microscopy and Microanalysis, IMA (Néode), HEI Arc.



Credit HE-Arc CR.

Fig. 6: Micrograph of the cross-section of Fig. 4 (detail), unetched, bright field. Light grey copper sulphide and tiny round Pb inclusions as well as "porosities" can be observed. Area of Fig. 10 is marked by a rectangle,

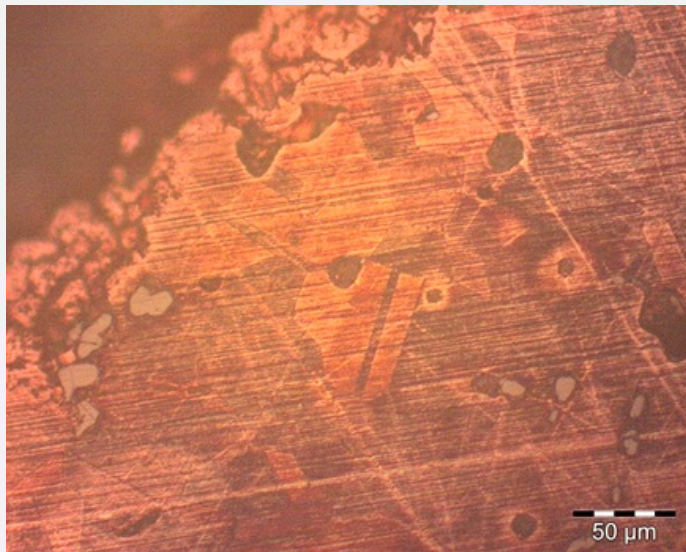


Credit HEI Arc_S.Ramseyer.

Fig. 7: SEM image, SE-mode, showing copper sulphide and lead inclusions,



Fig. 8: Micrograph of the metal sample from Fig. 4 showing a dendritic structure and grains,



Credit HE-Arc CR.

Fig. 9: Micrograph of a selected area showing grains and twin lines,

Microstructure	Dendritic structure & limited grain structure (with twin lines)
First metal element	Cu
Other metal elements	Sn, Pb

Complementary information

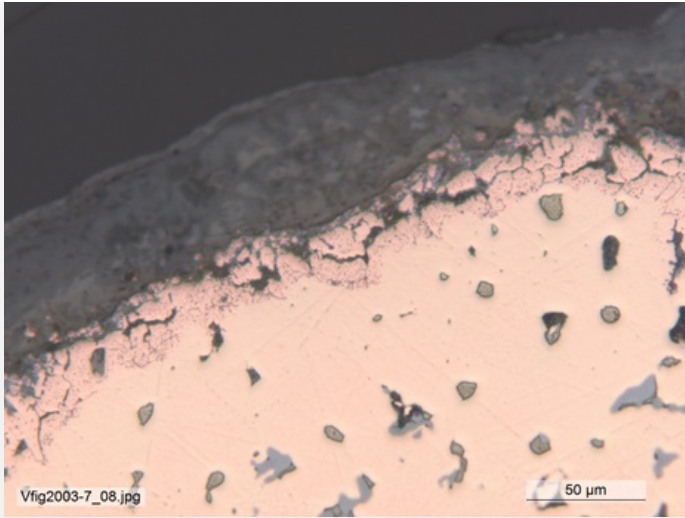
Nothing to report.

⌵ Corrosion layers

The remaining metal seems to have developed intergranular corrosion at the interface metal / corrosion layer (Fig. 10) slightly enriched in Sn (Fig. 12). The outer green corrosion product (CP2) is matte, powdery and mixed with sediments. It looks regular on Figs. 10 and 11 (around 50μm). This corrosion layer is mainly composed of lead (and/or sulphur), oxygen, silicon, chlorine and is depleted in Cu (Fig. 12 and table 2) except in its top part (CP1) where it is Cl, Cu and O-rich (Fig. 12 and table 2). FTIR seems to indicate that it is constituted of atacamite ($Cu_2Cl(OH)_3$, Fig. 13). This is confirmed on the EDS spectra of figure 14 where Pb is clearly detected. The inner black corrosion product (CP3) is a dark brown, matte layer (Figs. 2 and 11). It covers all the surface of the object, and forms a very thin layer. It is sulphur and oxygen-rich (Fig. 15). FTIR analysis could not reveal the presence of a specific corrosion product.

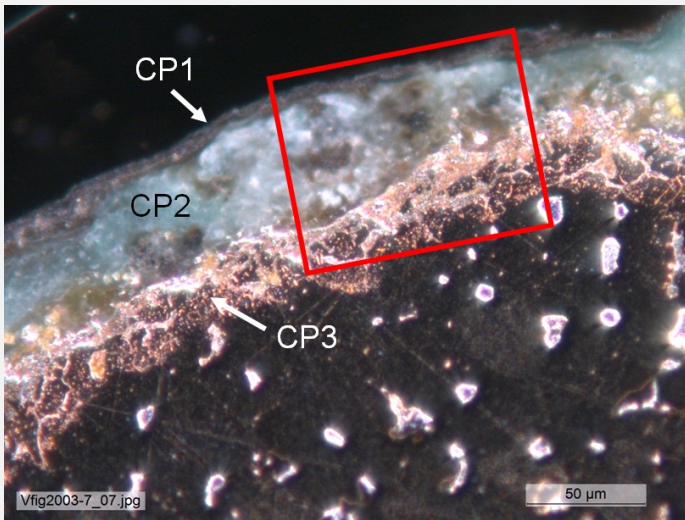
Elements proportions	O	Si	Cl	Pb/S	Cu	Sn
Blue corrosion product (CP1)	++	(+)	+	++	+	nd
Green corrosion product (CP2)	+	++	(+)	++	(+)	nd
Remnant metal phase	nd	nd	nd	+	++	++

Table 2: Chemical composition of the corrosion crust from Fig. 10. Method of analysis: SEM-EDS, Lab of Electronic Microscopy and Microanalysis, IMA (Néode), HEI Arc (+++: high concentration, ++ medium concentration, + low concentration, nd: not-detected).



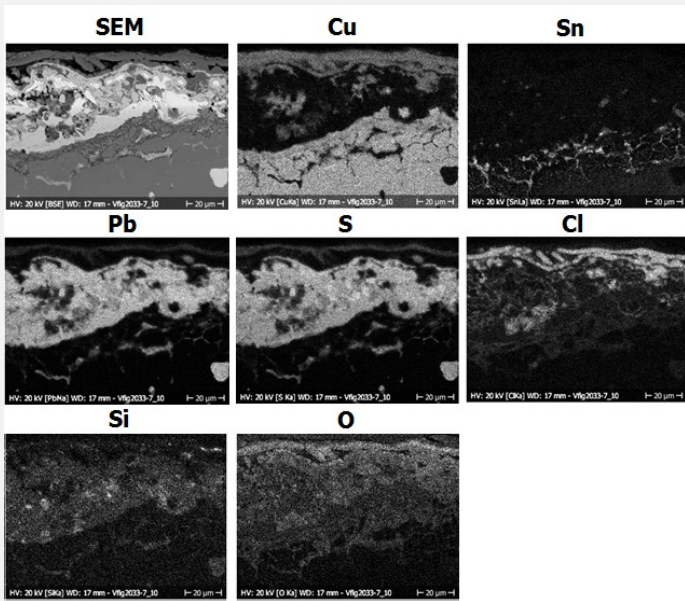
Credit HE-Arc CR.

Fig. 10: Micrograph of the metal sample from Fig. 6, unetched, bright field,



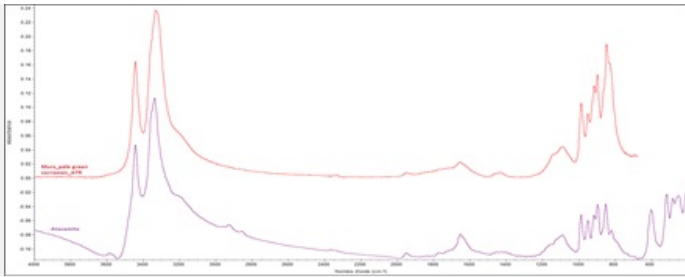
Credit HE-Arc CR.

Fig. 11: Micrograph similar to Fig. 10 and corresponding to the stratigraphy of Fig. 5, polarised light. The mapped area (Fig. 12, SEM) is marked by a rectangle,



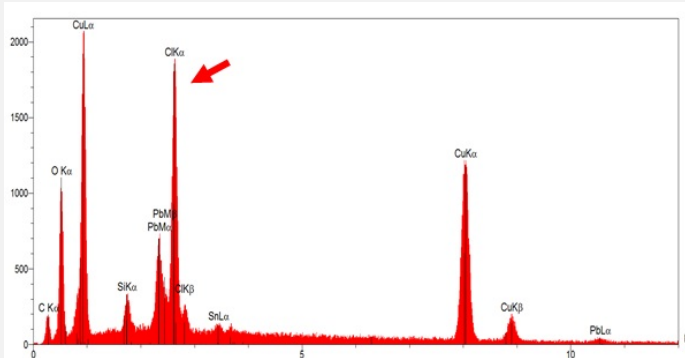
Credit HEI Arc, S.Ramseyer.

Fig. 12: SEM image, SE-mode, and elemental chemical distribution of the selected area of Fig. 11. Method of examination: SEM-EDS, Lab of Electronic Microscopy and Microanalysis, IMA (Néode), HEI Arc,



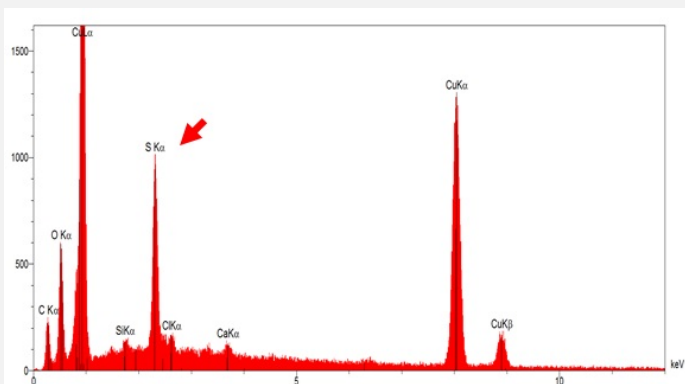
Credit HE-Arc CR.

Fig. 13: FTIR spectrum (ATR mode) of the green corrosion powder and comparison to atacamite (purple) spectrum. Method of analysis: FTIR spectroscopy, HE- Arc CR,



Credit HE-Arc CR.

Fig. 14: EDS analysis of the green corrosion powder (Fig. 2). Method of analysis: SEM-EDS, Lab of Electronic Microscopy and Microanalysis, IMA (Néode), HEI Arc,



Credit HE-Arc CR.

Fig. 15: EDS analysis of the black corrosion powder (Fig. 2). Method of analysis: SEM-EDS, Lab of Electronic Microscopy and Microanalysis, IMA (Néode), HEI Arc,

Corrosion form Uniform - intergranular
Corrosion type Artificial

Complementary information

Nothing to report.

✧ MiCorr stratigraphy(ies) – CS

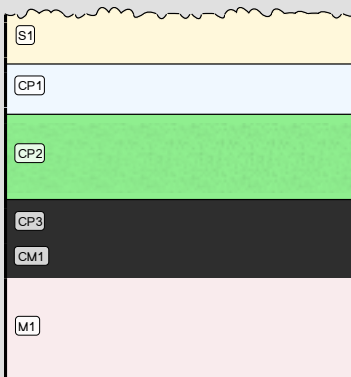


Fig. 5: Stratigraphic representation of the object in cross-section using the MiCorr application. This representation can be compared to Fig 11, Credit HE-Arc CR.

✧ Synthesis of the binocular / cross-section examination of the corrosion structure

Based on the analyses carried out, the schematic representation of the stratigraphy of corrosion layers has been corrected: a thin, black sulphur-rich layer covers the metal surface. A thick green layer has developed on top and seems to be constituted mainly of atacamite enriched in lead with sediments on top.

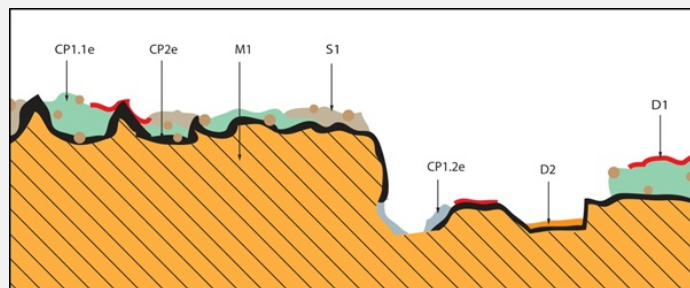


Fig. 16: Improved stratigraphic representation of the artefact from visual observations and analyses (additional mention e or i within the coding correspond to strata in contact with the environment (e) and internal strata (i),

Strata	Composition
Sediments (S1)	Si, O
Deposits (D1 & D2)	?
Outer green corrosion product (CP1e)	Atacamite
Inner black corrosion product (CP2i)	S, Cu, O
Remnant metal phase (M1)	Bronze (90%Cu, 10% Sn)

Credit HE-Arc CR, N.Barbezat.

✧ Conclusion

The artefact is a cast leaded bronze that has been partially annealed after cold working (surface finishing?). Strangely enough, one of the rolled up ends of the middle bar is filled with metal, testifying that it was cast already rolled-up. Normally it would have been rolled up after inserting the plates. The remaining metal seems to have developed intergranular corrosion limited to the interface metal / corrosion layers. The corrosion crust is constituted of an outer thick, green atacamite layer enriched in Pb and mixed with sediments while the inner thin, black corrosion layer is S, Cu and O-rich. This stratigraphy is unexpected for an archaeological artefact where we would expect chlorine to be at the interface metal / corrosion layer. Similarly, Si should be located on top layers although it was found deep in the outer green layer. Furthermore, S is found next to the metal surface while it should be present in higher concentrations in the top layers. Finally, Sn appears in an irregular and interrupted layer on top of the remaining metal. In an archaeological bronze it should be found as a clearly defined enriched layer. The red spots that looked like cuprite turned out to be paint. Since chlorine and sulphur are commonly used for the artificial patination of bronzes, we tend to conclude that this object is probably a fake produced during the 20th century.

✧ References

References on object and sample

Reference object

1. Houshang Mahboubian. Art of ancient Iran: Copper and Bronze. Philip Wilson, London, 1997.
2. Rickenbach, Judith. Magier mit Feuer und Erz. Museum Rietberg, Zürich, 1992.

References on analytic methods and interpretation

3. Craddock, P. (2009) Scientific investigation of copies, fakes and forgeries. Butterworth-Heinemann, Oxford.
4. Northover, P. (1997) "Appendix". In Houshang Mahboubian. Art of ancient Iran: Copper and Bronze. Philip Wilson, London, 325-338.
5. Oudbashi, O. and al. (2013) Micro-stratigraphical investigation on corrosion layers in ancient Bronze artefacts by scanning electron microscopy energy dispersive spectrometry and optical microscopy. Heritage Science, 1, 21.
6. Oudbashi, O. and al. (2014) Bronze in Archaeology: A Review of the Archaeometallurgy of Bronze in Ancient Iran". In INTECH [Online]. 2012 [consulted on february, the 21th 2014]. <http://www.intechopen.com/books/copper-alloys-early-applications-and-current-performance-enhancing-processes/bronze-in-archaeology-a-review-on-archaeometallurgy-of-bronze-in-ancient-iran>